Computation of the transmission loss of acoustic resonators

N. Wagner, R. Helfrich

INTES GmbH, Stuttgart, Germany
www.intes.de; info@intes.de

Summary:

Acoustic resonators have a large range of applications, e.g. in the intake and exhaust sections of combustion engines or the generation and playback of music. It is their task to filter out certain frequencies or a frequency band in order to attenuate the sound intensity as well as to effect the complex tone. An important measure for the assessment of the outcome of a resonator is the frequency dependent transmission loss.

Examples from the literature are used for comparison with experimental and numerical results based on FEM simulations. In the following all steps such as modeling, computation and evaluation, needed for computation of the transmission loss will be illustrated. It turns out to be a basic process that facilitates a fast comparison of different geometry variants with respect to the acoustic properties.

Zusammenfassung:

Akustische Resonatoren werden in vielen Anwendungsbereichen eingesetzt (u.a. im Ansaugtrakt und Abgasstrang von Verbrennungsmotoren oder bei Musikerzeugung und -wiedergabe). Ihre Aufgabe ist es, aus einem Schallfeld bestimmte Frequenzen oder ein Frequenzband herauszufiltern, um damit sowohl die Lautstärke als auch den Klang zu beeinflussen. Ein wichtiges Maß zur Beurteilung der Wirkung eines Resonators ist das frequenzabhängige Schalldämmmaß.

Zunächst werden Verifikationsbeispiele aus der Literatur vorgestellt und die Ergebnisse mit Finite-Elemente-Berechnungen verglichen. Anschließend werden ausgehend von einer gegebenen Geometrie des Resonators alle Schritte zur Ermittlung des Schalldämmmaßes mit finiten Elementen vorgestellt (wie Modellaufbau, Berechnung, Auswertung). Dabei zeigt sich ein einfacher Prozess, der für Geometrievarianten einen schnellen Vergleich des akustischen Verhaltens ermöglicht.

1 Introduction

Silencers with complicated internal acoustic components such as inlet/outlet tubes, thin buffles, perforated tubes, and sound absorbing materials have been introduced in automobiles, industrial equipments and environmental facilities [22]. The acoustic performance of a muffler may be evaluated using either the transmission loss (TL) or the insertion loss (IL), while the flow performance is evaluated using the pressure loss (PL), also named the backpressure [7]. IL values are preferred for most applications as a final design criteria [9], [23]. However we will focus on TL in this work. The transmission loss in decibels is defined as the difference between the incident sound power and transmitted sound power, assuming a reflection free termination. As long as the inlet and outlet regions of the silencer are of the same cross section, and the properties of the fluid (density, temperature) do not change, then the TL can be expressed as [9]:

$$TL = 20 \log_{10} \left| \frac{P_i}{P_{ref}} \frac{P_{ref}}{P_t} \right| = 20 \log_{10} \left| \frac{P_i}{P_t} \right| \tag{1}$$

where P_i and P_t denote the rms pressure of the incident and transmitted wave, respectively. $P_{ref} = 2 \cdot 10^{-5}$ Pa is a reference rms pressure value.

In case of 2D single expansion chambers the theoretical TL curve can be calculated by

$$TL = 10 \log_{10} \left[1 + \frac{1}{4} \left(m - \frac{1}{m} \right)^2 \sin^2 k \, L \right], \tag{2}$$

where m is the area ratio of inlet/outlet section to expansion chamber section and L denotes the length of the expansion chamber.

Different numerical techniques e. g. FEM [9], [18], [32], single and multi-domain BEM [12], [13], [26] Green's functions [29], Munjals's approach [20] and the transfer matrix method [24], [30] have been applied to the analysis and design of complicate acoustic systems. Most simulation studies in duct acoustics are using the transfer matrix method or the four-pole method, which is based on the assumption of plane wave propagation. This assumption is reasonable in the low-frequency region, which is relevant in many engine applications [6]. While analytical methods are applicable in case of simple geometries, numerical methods such as the finite element method are easy to be employed for acoustical systems with complex internal structures. They are also more flexible with respect to varying boundary conditions and material parameters.

Various experimental measurement techniques for the determination of the transmission loss are discussed in [21],[27], [28] and [33].

2 Governing Equations

The governing equations of the sound field is the linear time harmonic wave equation in three dimensions for acoustic pressure is given by

$$\nabla^2 p + k^2 p = 0, \quad k = \frac{\omega}{c}, \tag{3}$$

where ω is the angular frequency, k is the wave number, c is the speed of sound and p is the acoustic pressure. Different types of boundary conditions are available, e.g.

$$\frac{\partial p}{\partial n} = 0 \tag{4}$$

at the rigid walls of the chamber,

$$p = \bar{p}, \tag{5}$$

when a pressure source is assumed. The bulk modulus K of an acoustic medium is defined by

$$K = \rho \, c^2. \tag{6}$$

Flow effects have been neglected and can be found elsewhere [10].

3 Visper

VisPER (Visual PERMAS) is a GUI based model editor [3]. It is used to complete finite element models for specific applications with PERMAS [1]. To this end VisPER fills efficiently the gap between FE models generated by a standard pre-processor such as Medina [5], and PERMAS [4] models which are ready to run. VisPER can also be used for model verification and post-processing tasks.

3.1 FS Wizard

A wizard establishes a workflow for a model completion task. The wizard is aimed to guide the user step-by-step through the different steps, which are given below:

- **Basics**:
  First, the fluid material is defined through the density and compressibility of the fluid.defined according to the requirements of the model such as the size of internal holes or the highest frequency to be considered. In addition, a recommended mesh size is calculated based on a frequency range for subsequent analysis.

- **Hole detection**:
  Hole detection is performed automatically. Only those holes are detected which are larger than the previously specified mesh size. The hole detection algorithm adopted here searches for free element edges, i.e. element edges belonging to only one 2D-element. A hole is then a closed path of free element edges.

- **Hole definition**:
  Due to difficult topological situations, some holes cannot be detected automatically. Therefore, undetected holes may be specified in addition.

- **Hole meshing**:
  Hole meshing is performed automatically. For this purpose special elements (PLOTA3, PLOTA4) are used which do not introduce any mass or stiffness. They are just used to define the topology of the corresponding hole and to limit the subsequent cavity meshing process.

- **Mesh generation**:
  Perform the fluid meshing process.The basic fluid mesh is a hierarchical voxel mesh, that grows from an interior seed point towards the outer structural mesh. The voxel mesh is being completed by appropriate elements (FLTET4, FLPYR5, FLPENT6) at the structural mesh surfaces.

- **Relaxation**:
  When meshing is finished, there are some elements penetrating the hull of the cavity. These penetrations are resolved by a relaxation process which performed automatically.

- **FS coupling**:
  Finally, the interface elements and the MPC conditions are created to establish the coupling conditions between fluid and structure meshes. The nodes of these interface elements have both pressure and displacement degrees of freedom.

4 Examples

The speed of sound used in the computational study is 346.1 m/s at $T = 25°$ C. A uniform velocity excitation is imposed at the inlet section of the muffler. To apply velocity type boundary conditions, interface elements are used in PERMAS (FSINTA3,FSINTA4). The velocity boundary condition is converted to a displacement using the relationship

$$u = \hat{u} \exp(i\Omega t), \quad v = \dot{u} = i\Omega \hat{u} \exp(i\Omega t). \tag{7}$$

The inlet boundary condition can thus be specified with a velocity magnitude equal to unity. These interface elements are applied at the inlet section of the muffler. An impedance

$$z = \rho_0 \, c \tag{8}$$

is applied to the outlet end to simulate anechoic termination. This condition is realized by adding *Enquist-Majda* elements (denoted by RBCEM1A3, RBCEM1A4 in PERMAS) at the outlet section.
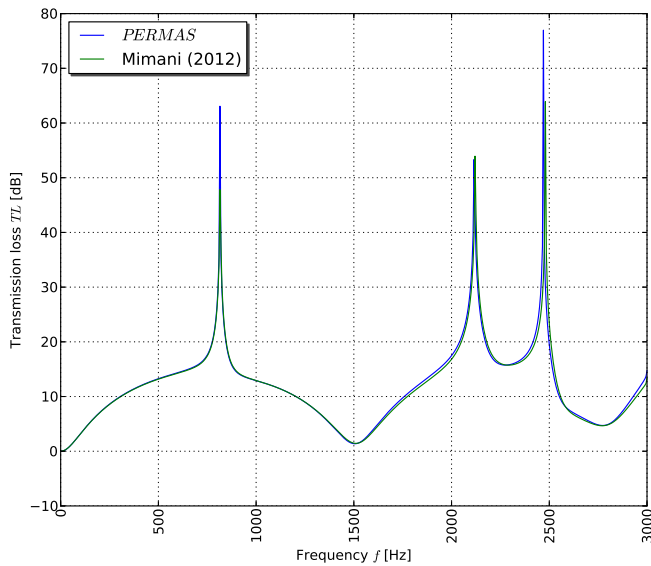
4.1 Short chamber

The first example is taken from [19]. The speed of sound is taken as c_0=343.1382 ms^{-1} in the first two examples. The major and minor axis of the elliptical chamber D_1 and D_2 respectively as well as the port diameters of the end inlet d_E and side outlet d_S are fixed as $D_1 = 0.25$m, D_2=0.15m and $d_E = d_S = 0.04$m. The side walls are rigid so that the normal pressure gradient (4) vanishes.
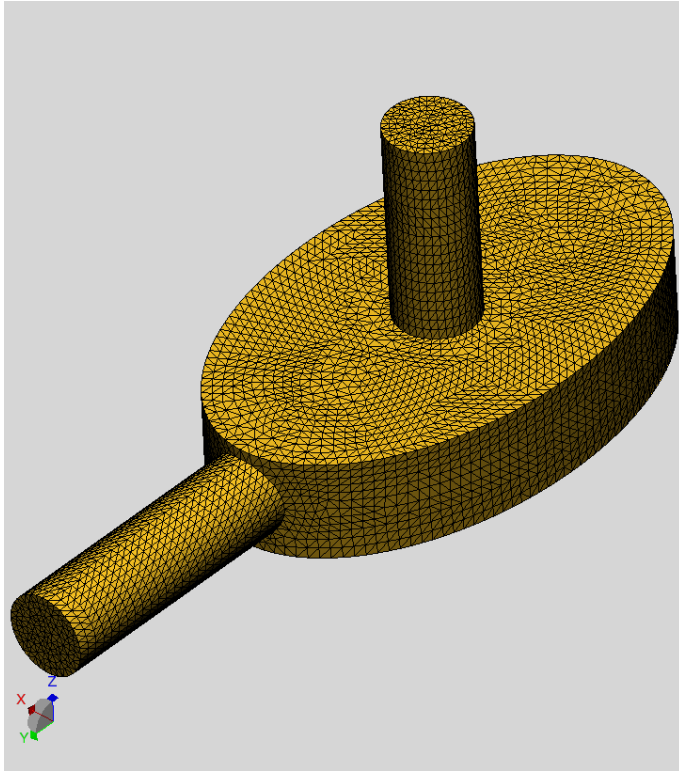
**Fig. 1: Surface mesh of a short chamber** $L = 0.05$**m**

The transmission loss curves are compared in Figure 2. A perfect agreement over the whole frequency range is visible.

Fig. 2: Transmission loss for an axially short chamber $L = 0.05$**m**

4.2 Long chamber

The second example is also taken from [19]. The mesh is depicted in Figure 3. Again the numerical results of PERMAS are in good accordance with the results of Mimani Figure 4.
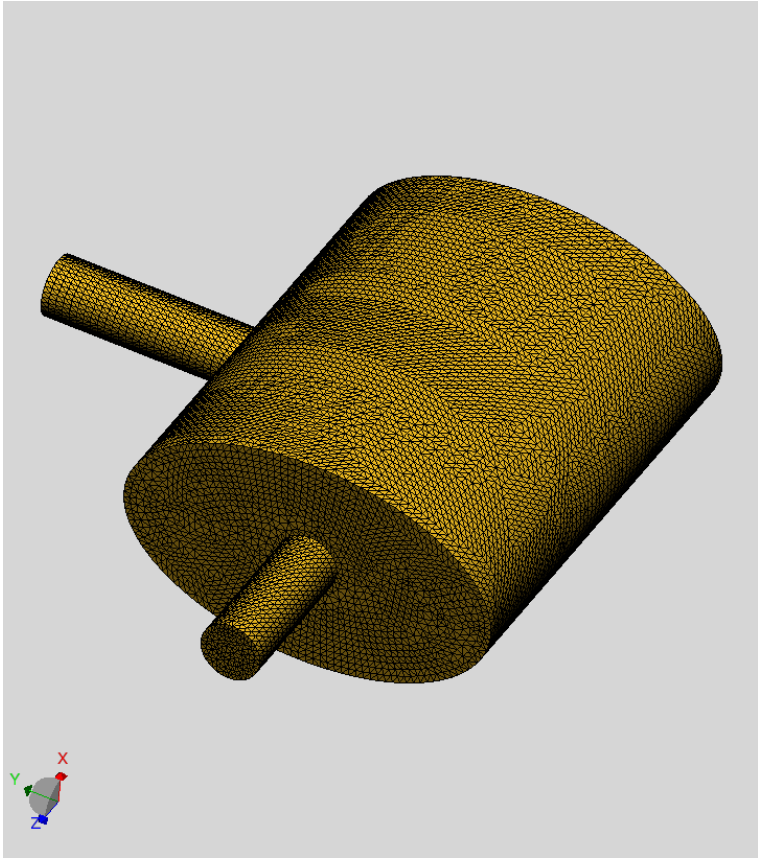
Fig. 3: Mesh of a long chamber $L = 0.3$**m**
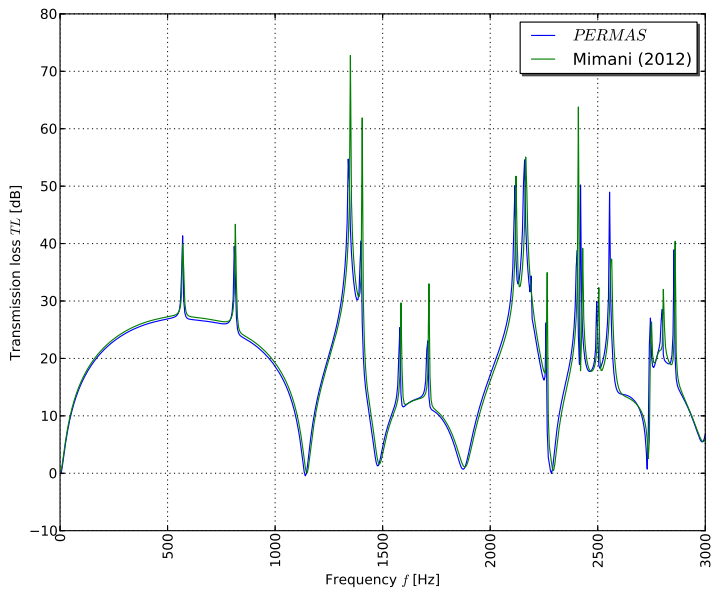
Fig. 4: Transmission loss of an axially long elliptic chamber $L = 0.3$**m**
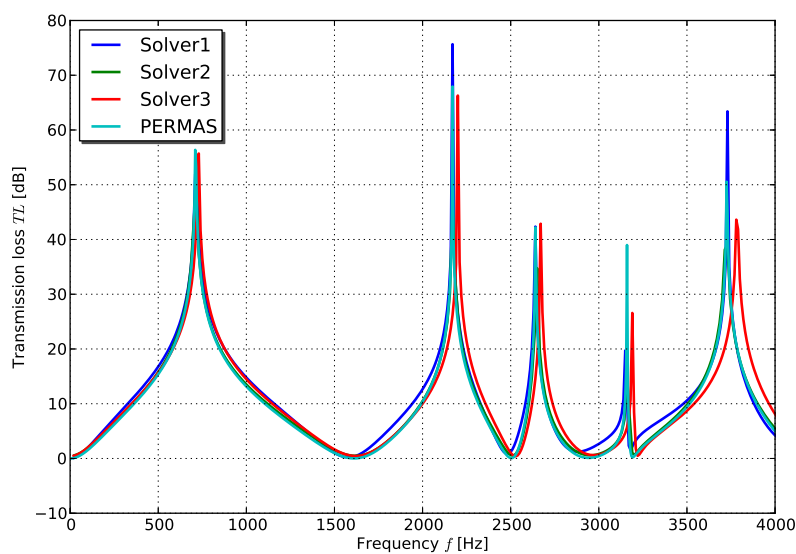
4.3   Single chamber design

The following three examples are taken from [14],[15]. They have compared several commercial acoustic FEA software. To fill the gap the results by PERMAS have been added for completeness. All computations have been carried in the direct frequency domain. However, PERMAS is also able to conduct the analyses in the modal

domain. The modal basis may be enriched by additional static mode shapes. Compressible and incompressible fluids can be handled by PERMAS. The first model is illustrated in Figure 5.
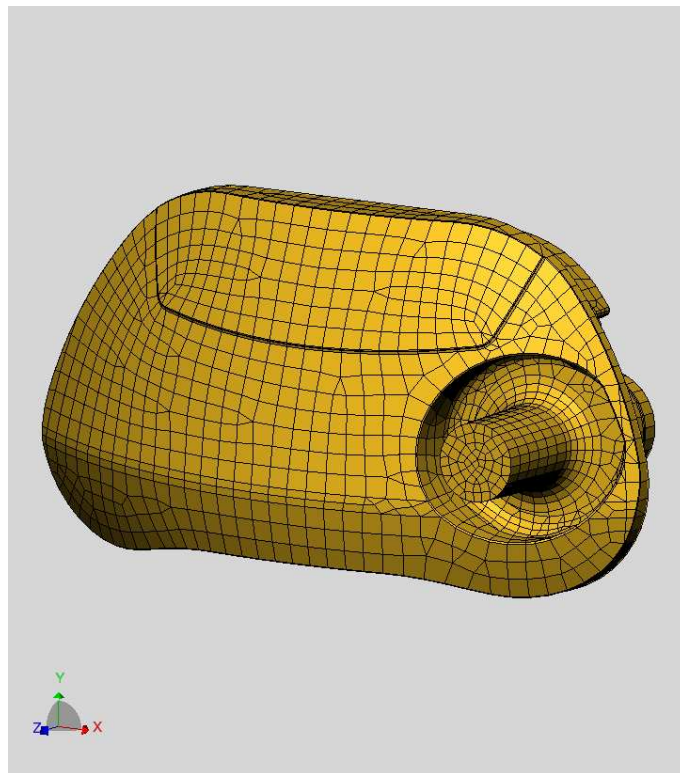

Fig. 5: Model of the single chamber $L = 0.05$m

Figure 6 compares the transmission loss results obtained for the short chamber by using different solvers. There are no result for one competitor since it was not possible to generate a suitable mesh in that case [14]. That is due to the quality of the underlying geometry with many intersecting curved surfaces. Some slight deviations between the different curves become apparent, especially for higher frequencies. Several reasons, such as different element types, meshes and varying approaches come into consideration. Altogether the global behaviour is predicted very well.
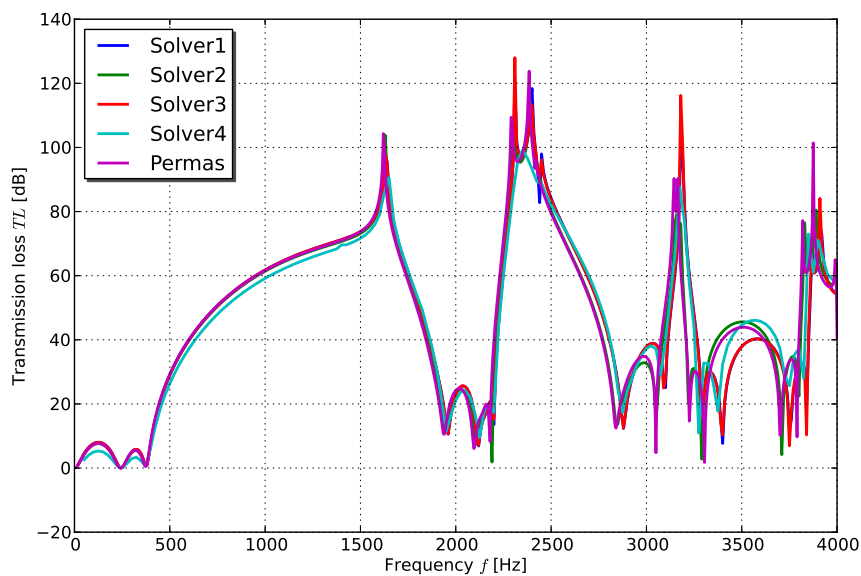

Fig. 6: Transmission loss for a single chamber design

4.4 Interconnected chamber design

The mesh of the interconnected chamber is depicted in Figure 7.
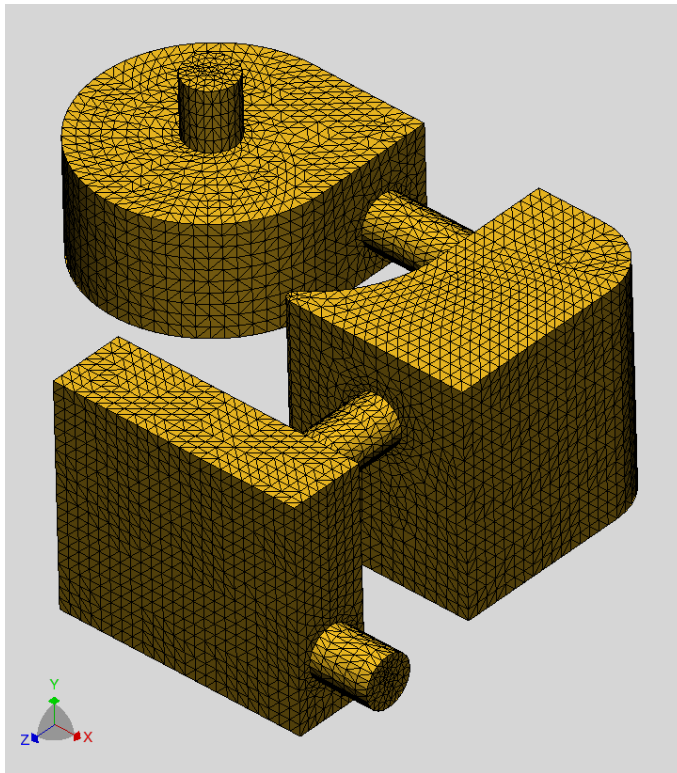
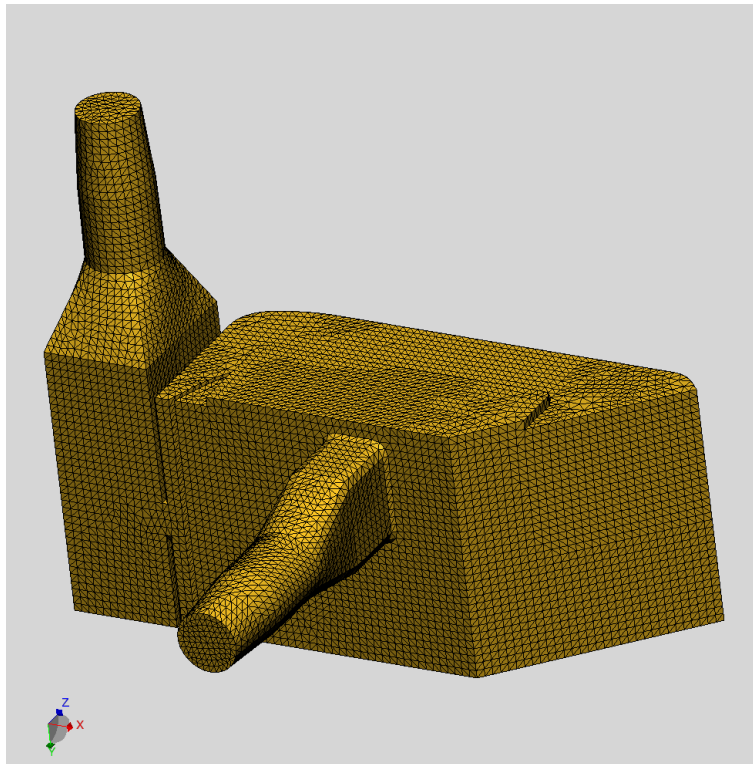**Fig. 7: Surface mesh of the interconnected chamber**

Fig. 8: Transmission loss for an interconnected chamber design

Figure 8 compares the transmission loss results obtained for the interconnected chamber muffler using different FE modelling software packages. The deviations increases with frequency. The predicted resonance frequencies match very well.
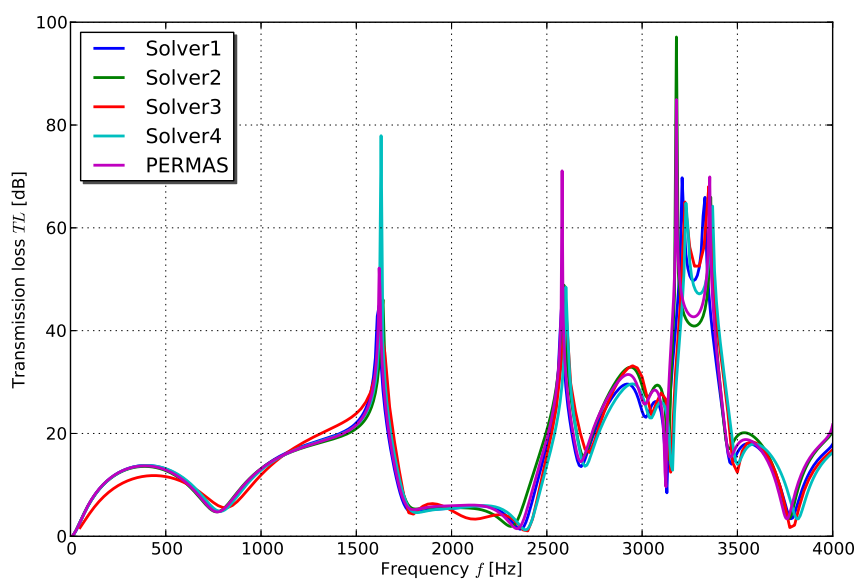
4.5 Integrated chamber design

Figure 9 illustrates the mesh of the integrated chamber.

**Fig. 9: Surface mesh of the integrated chamber**

Figure 10 compares the transmission loss results obtained for the integrated chamber muffler using different FE modelling software packages. Again a good agreement is visible although one commercial solver yields deviations even in the low frequency range.


Fig. 10: Transmission loss for an integrated chamber design

4.6 Industrial application

The last example is an industrial application. The hexahedral-dominant mesh generated by Visper is depicted in Figure 11. The element size clearly decreases in the vicinity of the surface layer and the coupling links between the different chambers of the resonator Figure 13. Interpolation elements (IQUAD4) are used in the transitions regions in order to couple incompatible parts of the solid mesh.
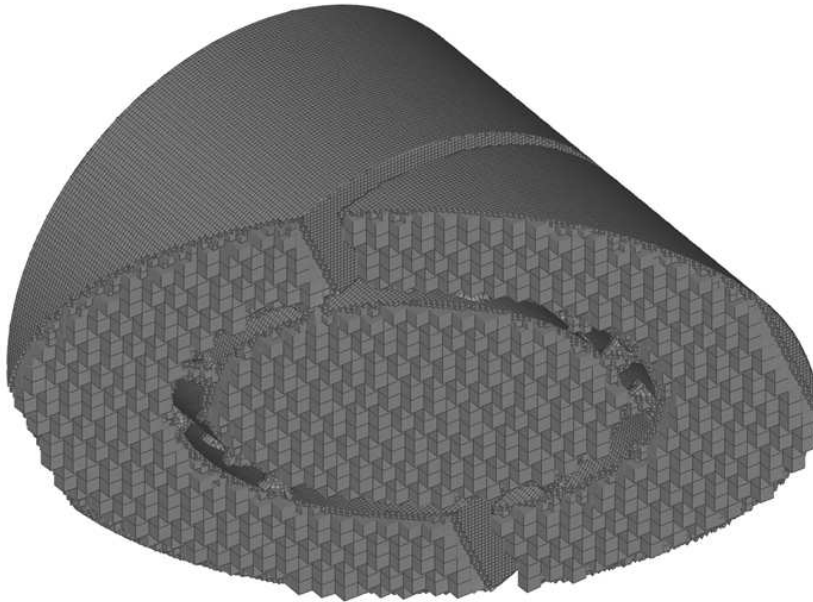
Fig. 11: Section of a hexahedral-dominant fluid mesh of the resonator
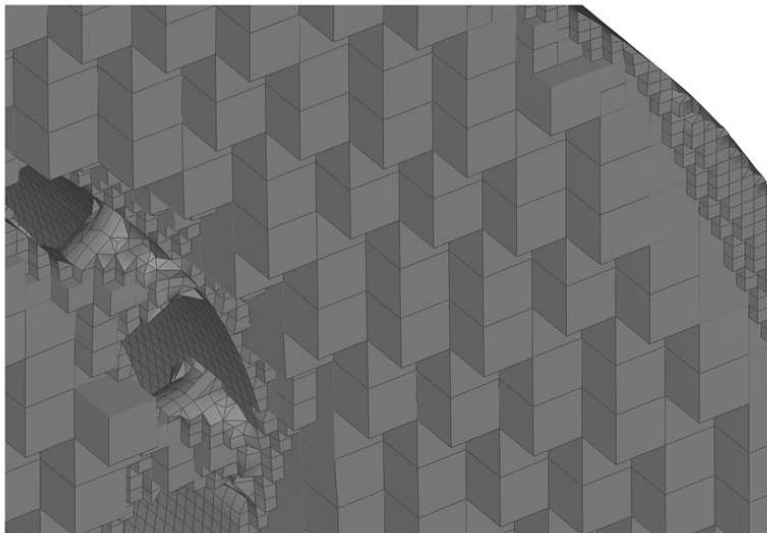

Fig. 12: Detail of Figure 11
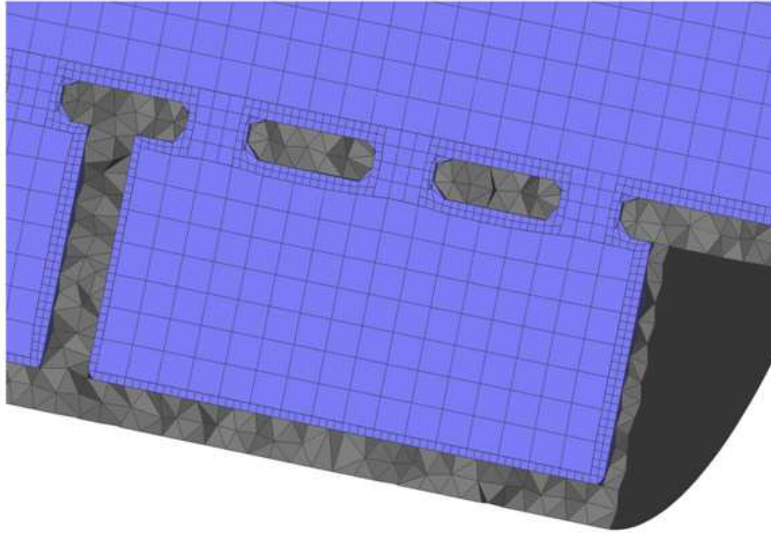
Fig. 13: Section of a hexahedral-dominant mesh of the resonator: blue - fluid part; grey - structural part

Figure 14 illustrates the transmission loss curves obtained for the industrial resonator. It should be noted that PERMAS can handle different analyses types with one model, that is the structural part is simply neglected in a pure fluid vibration analysis and vice versa. The structure consists of plastic material ($E = 2320$MPa, $\nu = 0.3, \rho = 1040$kg/m^3).
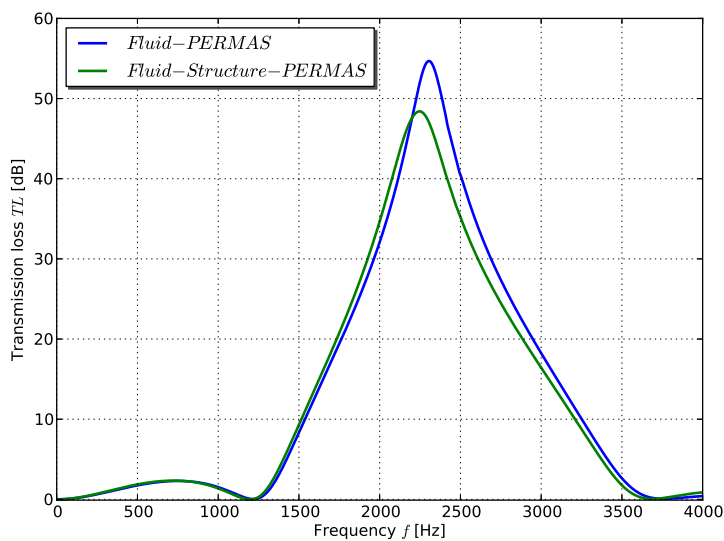
Fig. 14: Transmission loss for an industrial resonator

5 Conclusions

The acoustic behaviour of different chambers is examined in terms of transmission loss. 3D simulations in PER-MAS of different chamber configurations are performed and compared with results from the literature.

Possible extensions of the presented material include:

- The internal partition configuration of a resonator affects significantly its acoustical transmission characteristics. For this reason it becomes obvious to use topology optimization of muffler internal partitions for improving acoustical attenuation performance [16], [17].

- Shape optimization for getting optimized positions of inlet/outlet is studied in [6], [8]. In that context Airaksinen [6] introduced a multiobjective optimization problem for acoustic mufflers. It is defined to maximize the TL at two frequency ranges simultaneously. The open-source Netgen mesh generator by Schöberl [25] is used to create tetrahedral meshing of the (updated) muffler geometry. Yeh et. al. [31] applied simulated annealing and a genetic algorithm in the shape optimization of double-chamber mufflers.

These topics will be investigated in the near future.

6   Acknowledgment

References

[1] *PERMAS Version 14: Users' Reference Manual*, INTES Publication No. 450, Stuttgart, 2012.

[2] *PERMAS Version 14: Examples Manual*, INTES Publication No. 550, Stuttgart, 2012.

[3] *Visper Version 3.1.005: Visper Users Manual*, INTES Publication No. 470, Stuttgart, 2012.

[4] *PERMAS Product Description Version 14*, INTES, Stuttgart, 2012,
http://www.intes.de/kategorie_unternehmen/publikationen

[5] *Medina FEM Pre- and Post-Processing*, T-Systems International GmbH, http://servicenet.t-systems.com/medina

[6] T. Airaksinen, E. Heikkola: *Multiobjective muffler shape optimization with hybrid acoustics modeling*, J. Acoust. Soc. Am., Vol. 130, pp. 1359–1369, 2011.

[7] K. S. Andersen: *Analyzing muffler performance using the transfer matrix method*, Excerpt from the Proceedings of the COMSOL conference, Hannover 2008.

[8] R. Barbieri, N. Barbieri: *Finite element acoustic simulation based shape optimization of a muffler*, Applied Acoustics, Vol. 67, pp. 346–357, 2006.

[9] S. Bilawchuk, K. R. Fyfe: *Comparison and implementation of the various numerical methods used for calculating transmission loss in silencer systems*, Applied Acoustics, Vol. 64, pp. 903–916, 2003.

[10] P. Choudary Chaitanaya, M. L. Munjal: *Tuning of the extended concentric tube resonators*, International Journal of Acoustics and Vibration, Vol. 16, pp. 111–118, 2011.

[11] C. I. Chu, H.T. Hua, I.C. Liao: *Effects of three-dimensional modes on acoustic performance of reversal flow mufflers with rectangular cross-section*, Computers and Structures, Vol. 79, pp. 883–890, 2001.

[12] X. B. Cui, Z. L. Ji: *Fast multipole boundary element approaches for acoustic attenuation prediction of reactive silencers*, Engineering Analysis with Boundary Elements, Vol. 36, pp. 1053–1061, 2012.

[13] Z. L. Ji: *Boundary element acoustic analysis of hybrid expansion chamber silencers with perforated facing*, Engineering Analysis with Boundary Elements, Vol. 34, pp. 690–696, 2010.

[14] P. Jones, N. Kessissoglou: *An evaluation of current commercial acoustic FEA software for modelling small complex muffler geometries: prediction vs experiment* Proceedings of Acoustics, 22-25 November 2009, Adelaide, Australia.

[15] P. W. Jones, N. J. Kessissoglou: *A numerical and experimental study of the transmission loss of mufflers used in respiratory medical devices*, Acoustics Australia, Vol. 38, pp. 13–19, 2010.

[16] J. W. Lee, Y. Y. Kim: *Topology optimization of muffler internal partitions for improving acoustical attenuation performance*, International Journal for Numerical Methods in Engineering, Vol. 80, pp. 455–477, 2009.

[17] J. W. Lee, G.-W. Jang: *Topology design of reactive mufflers for enhancing their acoustic attenuation performance and flow characteristics simultaneously*, International Journal for Numerical Methods in Engineering, Vol. 91, pp. 552–570, 2012.

[18] O. Z. Mehdizadeh, M. Paraschivoiu: *A three-dimensional finite element approach for predicting the transmission loss in mufflers and silencers with no mean flow*, Applied Acoustics, Vol. 66, pp. 902–918, 2005.

[19] A. Mimani, M. L. Munjal: *3-D acoustic analysis of elliptical chamber mufflers having an end-inlet and a side-outlet: An impedance matrix approach*, Wave Motion, Vol. 49, pp. 271–295, 2012.

[20] M. L. Munjal: *A simple numerical method for three-dimensional analysis of simple expansion chamber mufflers of rectangular as well as circular cross-section with a stationary medium*, Journal of Sound and Vibration, Vol. 116, pp. 71–88, 1987.

[21] O. Olivieri, J. S. Bolton, T. Yoo: *Measurement of transmission loss of materials using a standing wave tube*, Inter-Noise, Honolulu, Hawaii pp. 5285–5292, 2006.

[22] Y.-B. Park, H.-D. Ju, S.-B. Lee: *Transmission loss estimation of three-dimensional silencers by system graph approach using multi-domain BEM*, Journal of Sound and Vibration, Vol. 328, pp. 575–585, 2009.

[23] B. Rajavel, M. G. Prasad: *Technical Note: Effects due to Exhaust and Tail Pipes on Insertion Loss of Mufflers*, International Journal of Acoustics and Vibration, Vol. 16, pp.98–100, 2011.

[24] A. D. Sahasrabudhe, S. A. Ramu, M. L. Munjal: *Matrix condensation and transfer matrix techniques in the 3-D analysis of expansion chamber mufflers*, Journal of Sound and Vibration, Vol. 147, pp. 371–394, 1991.

[25] J. Schöberl: *NETGEN - An advancing front 2D/3D-mesh generator based on abstract rules*, Comput. Visual. Sci., Vol. 1, pp. 41–52, 1997.

[26] A. Selamet, Z. L. Ji: *Acoustic attenuation performance of circular expansion chambers with extended inlet/outlet*, Journal of Sound and Vibration, Vol. 223, pp. 197–212, 1999.

[27] A. F. Seybert, D. F. Ross: *Experimental determination of acoustic properties using a two-microphone random excitation technique*, Journal of the Acoustical Society of America, Vol. 61, pp. 1362–1370, 1977.

[28] Z. Tao, A. F. Seybert: *A Review of Current Techniques for Measuring Muffler Transmission Loss*, Noise & Vibration Conference and Exhibition, Traverse City, Michigan, May 5-8, 2003.

[29] B. Venkatesham, M. Tiwaru, M. L. Munjal: *Transmission loss analysis of rectangular expansion chamber with arbitrary location of inlet/outlet by means of Green's functions*, Journal of Sound and Vibration, Vol. 323, pp. 1032–1044, 2009.

[30] N. K. Vijayasree, M. L. Munjal: *On an integrated transfer matrix method for multiply connected mufflers*, Journal of Sound and Vibration, Vol. 331, pp. 1926–1938, 2012.

[31] L.-J. Yeh, Y.-C. Chang, M.-C. Chiu: *Shape optimal design on double-chamber mufflers using simulated annealing and a genetic algorithm*, Turkish J. Eng. Env. Sci., Vol. 29, pp. 207–224, 2005.

[32] C. J. Young, M. J. Crocker: *Prediction of transmission loss in mufflers by the finite element method*, Journal of the Acoustical Society of America, Vol. 57, pp. 144–148, 1975.

[33] S. Zheng, C. Kleinfeld: *Transmission loss measurement with and without an anechoic termination*, SAE 2009 Noise and Vibration Conference, SAE 2009-01-2035.